Received: 29 October 2017 | Revised: 7 June 2018 | Accepted: 7 July 2018

DOI: 10.1002/ajpa.23688

WILEY American Journal of PHYSICAL ANTHROPOLOGY

RESEARCH ARTICLE

Do forelimb shape and peak forces co-vary in strepsirrhines?

Anne-Claire Fabre[1,2] | Michael C. Granatosky[3] | Jandy B. Hanna[4] | Daniel Schmitt[1]

[1]Department of Evolutionary Anthropology, Duke University, Durham, North Carolina

[2]UMR 7179 C.N.R.S., M.N.H.N. Département Adaptations du Vivant, Muséum National d'Histoire Naturelle, Paris, France

[3]Department of Organismal Biology and Anatomy, University of Chicago, Chicago, Illinois

[4]Department of Biomedical Science, West Virginia School of Osteopathic Medicine, Lewisburg, West Virginia

Correspondence
Anne-Claire Fabre, UMR 7179, Département d'Ecologie et de Gestion de la Biodiversité, Museum National d'Histoire Naturelle, 57 rue Cuvier, Case Postale 55, 75231, Paris Cedex 5, France.
Email: anne-claire.fabre@mnhn.fr

Funding information
Fondation Fyssen; Force and Motion Foundation; Leakey foundation; Marie-Skłodowska Curie, Grant/Award Number: EU project 655694 - GETAGRIP; National Science Foundation, Grant/Award Number: NSF BCS 0749314

Abstract

Objectives: In this study, we explore whether ground reaction forces recorded during horizontal walking co-vary with the shape of the long bones of the forelimb in strepsirrhines. To do so, we quantify (1) the shape of the shaft and articular surfaces of each long bone of the forelimb, (2) the peak vertical, mediolateral, and horizontal ground reaction forces applied by the forelimb during arboreal locomotion, and (3) the relationship between the shape of the forelimb and peak forces.

Materials and methods: Geometric morphometric approaches were used to quantify the shape of the bones. Kinetic data were collected during horizontal arboreal walking in eight species of strepsirrhines that show variation in habitual substrate use and morphology of the forelimb. These data were then used to explore the links between locomotor behavior, morphology, and mechanics using co-variation analyses in a phylogenetic framework.

Results: Our results show significant differences between slow quadrupedal climbers (lorises), vertical clinger and leapers (sifaka), and active arboreal quadrupeds (ring-tailed lemur, ruffed lemur) in both ground reaction forces and the shape of the long bones of the forelimb, with the propulsive and medially directed peak forces having the highest impact on the shape of the humerus. Co-variation between long bone shape and ground reaction forces was detected in both the humerus and ulna even when accounting for differences in body mass.

Discussion: These results demonstrate the importance of considering limb-loading beyond just peak vertical force, or substrate reaction force. A re-evaluation of osseous morphology and functional interpretations is necessary in light of these findings.

KEYWORDS

covariation, geometric morphometrics, locomotion, peak forces, primate

1 | INTRODUCTION

It has long been argued that the mechanical demands of different locomotor modes impact the shape and design of the musculoskeletal system (see Smith & Savage, 1956; Biewener, 1983a, 2005 for a review). It is widely assumed that limb long bone shape has evolved to resist and transfer mechanical loads during locomotion (Currey, 2002) while avoiding mechanical failure. But the specific aspects of loading (i.e., peak force, impulse, frequency, strain rate) and the specific cellular physiology that drive bone formation remain an area of considerable contention (see Huiskes & van Rietbergen, 2005; Lanyon & Rubin, 1985; Ruff, Holt, & Trinkaus, 2006; Schmitt, Zumwalt, & Hamrick, 2010; Hylander & Johnson, 1997 for general reviews and those specific to small mammals and primates). This is an area of research that is vital to paleoanthropology, as establishing mechanical relationships between form (bone shape) and the external environment (loading in this case) are essential to reconstructing behavior in extinct primates (Arnold, 1983).

During locomotion, limb bones are subject to external forces including substrate reaction forces and muscle forces. Previous studies have shown that variation in bone architecture and shape (Alexander, 1980, 1996; Currey, 2002; Fabre, Marigó, Granatosky, & Schmitt, 2017; Hildebrand, 1985; Lee & Lanyon, 2004; Lieberman & Pearson, 2001; Smith & Savage, 1956) reflect aspects of locomotor behavior. However, the link between the shape of the bone and external forces acting on it during locomotion remains poorly understood, in part because few prior studies have included explicit comparisons of both sets of data. In addition, during ontogeny and throughout an animal's life, bone is modeled and remodeled. It has been argued that

remodeling reflects the stresses caused by torsion and bending during locomotion (Allan, Cassey, Snelling, Maloney, & Seymour, 2014; Burr, 2002; Currey, 2003; Lee, Staines, & Taylor, 2003; Lieberman, Pearson, Polk, Demes, & Crompton, 2003; Main & Biewener, 2004; Robling, Castillo, & Turner, 2006; Robling, Hinant, Burr, & Turner, 2002). Furthermore, it has been argued that phylogeny may have as large or possibly a larger influence than external forces on at least some aspects of limb bone shape (Walmsley et al., 2012). Thus, the association between bone shape and external factors remains complex and it is not always clear to what degree overall bone shape is influenced by external forces in the adult animal, behavioral changes over ontogeny that lead to differences in external forces, and/or phylogeny.

Although there is extensive debate about the factors that influence bone anabolism (e.g., Bertram & Swartz, 1991; Main & Biewener, 2007; Martin & Burr, 1982; Rubin, Gross, Donahue, Guilak, & McLeod, 1994), it is clear that ground reaction forces generated during locomotion play an important role in the overall loading environment for any long bone (Bertram & Biewener, 1988; Biewener, 1983a; Rubin & Lanyon, 1984). But there remain good theoretical and empirical reasons to be skeptical of the simplistic assumption of a straight-forward relationship, independent of phylogeny, between bone shape and loading pattern (Huiskes & van Rietbergen, 2005; Lanyon & Rubin, 1985). This is in part because of a lack of strict phylogenetically controlled associations and information on how loading influences bone shape at a cellular level. This study addresses the first part of that problem. Although, numerous studies of large and medium-sized animals such as horses, dogs, and primate have provided important insights into the relationship between bone strength and loading (Biewener, 1982, 1983a, 1983b, 1989, 1991; Blob & Biewener, 2001; Budsberg, Verstraete, & Soutas-Little, 1987; Carlson, Demes, & Franz, 2005; Demes et al., 1998; Demes, Qin, Stern, Larson, & Rubin, 2001; Merkens, Schamhardt, van Osch, & Bogert, 1993a; Merkens, Schamhardt, van Osch, & Hartman, 1993b; Riggs, Vaughn, Evans, Lanyon, & Boyde, 1993), no studies have examined a wide variety of locomotor modes in a phylogenetic context and included the actual forces engendered during movement.

To fill this critical gap and to contribute to an understanding of form-function relationships in extant and extinct primates, we examine the relationship between the shape of the long bones of the forelimb and the peak external forces acting on them during arboreal locomotion (walking on a horizontal pole) in a comprehensive sample of strepsirrhine primates. This group provides an ideal sample for a study of this kind because they utilize a wide array of arboreal and terrestrial substrates (Fleagle, 2013; Oxnard, Crompton, & Lieberman, 1990). Additionally, they display broad variation in the use and morphology of the forelimb (Gebo, 1987; Martin, 1974) ranging from quadrupeds that move often on the ground (ring-tailed lemur) to those that are exclusively arboreal (e.g., brown lemurs, aye-ayes, and ruffed-lemurs), to those that are vertical clinger and leapers (sifakas, bamboo lemurs), and others that are habitually slow, suspensory climbers (lorisids). Here, locomotor peak forces during arboreal quadrupedal locomotion are compared. Arboreal quadrupedal locomotion is a locomotor type used by all species in this sample and is often considered the basal locomotor mode for primates (Hunt et al., 1996; Rose, 1973). Furthermore, it is well-characterized mechanically in primates (Demes et al., 1994; Franz, Demes, & Carlson, 2005; Granatosky, Tripp, & Schmitt, 2016a; Hildebrand, 1967; Kimura, Okada, & Ishida, 1979; Larson, Schmitt, Lemelin, & Hamrick, 2000; O'Neill & Schmitt, 2012; Schmitt, 1999; Vilensky & Larson, 1989). However, little is known about the quadrupedal movements of primates that regularly engage in other, more specialized, forms of locomotion (e.g., leaping or suspensory locomotion, but see Granatosky, Tripp, & Schmitt, 2016a and Granatosky & Fitzsimons, 2017), or have specialized morphology that could influence quadrupedal gait characteristics (e.g., long hind limbs, elongated and often slender digital rays; Krakauer et al., 2002; Kivell et al., 2010). Thus, we are asking how variation in single limb peak substrate reaction forces during arboreal quadrupedal locomotion affects forelimb long bone shape in primates.

From a simple anatomical and mechanical perspective, it is reasonable to expect that peak forces on the forelimb during locomotion will impact all three-upper limb long bones. Moreover, we predict that vertical peak forces, rather than fore-aft or mediolateral forces, will have the highest impact on the robusticity and the shape of the forelimb long bones during locomotion on horizontal branches (Riskin, Bertram, & Hermanson, 2005). This is because vertical force tends to be the highest contributor to overall substrate reaction forces (Demes et al., 1994). Therefore, we expect peak vertical force and bone shape to vary in predictable ways in association with both body mass and locomotor specialization. It is also possible that variation in fore-aft or mediolateral forces may also be related to limb bone shape, but predictions are more difficult to make due to our lack of understanding of the variation and magnitude of these forces during horizontal branch walking (Carlson et al., 2005; Schmitt, 2003; Granatosky, Fitzsimons, Zeininge & Schmitt, 2018). Alternatively, the different locomotor modes (e.g., slow-quadrupedal walking, vertical clinging and leaping, active arboreal quadrupedalism) of the species included in our study may drive limb shape to a greater extent than the peak forces. For example, the body form associated with habitual locomotor behavior like vertical clinging and leaping may influence the ground reaction forces during quadrupedal branch walking (Granatosky, Tripp, Fabre, & Schmitt, 2016b). Phylogenetic history may be an additional and relevant confounding factor. With all of this in mind, we explore covariation between limb long bone shape and ground reaction forces while taking phylogeny and habitual locomotor mode into account.

2 | MATERIAL AND METHODS

2.1 | Osteological sample and data collection

The morphological data set is composed of the humerus, ulna, and radius from 35 individuals belonging to one species of Daubentoniidae, one species of Indriidae, four species of Lemuridae, and two species of Lorisidae (Table 1, Supporting Information Table S1). For each species, the number of osteological specimens ranged from 2 to 6 (Table 1). In most cases, osteological specimens were of wild caught origin, and equal numbers of males and females were included where possible. Specimens were obtained from the collection of the Anatomie Comparée, Muséum National d'Histoire Naturelle (MNHN), Paris, France (See Supporting Information Table S1 for a complete list of the

TABLE 1 Specimens used in the analyses with family, species name, and number of individuals included in the shape analysis (Ns) and in the kinetic analysis (Nk)

Family	Species	Locomotor behavior	Ns	Nk	Substrate diameter (cm)
Daubentoniidae	*Daubentonia madagascariensis*	Active quadrupedalism	4	2	3.18
Indriidae	*Propithecus coquereli*	Vertical clinging and leaping	5	3	3.18
Lemuridae	*Eulemur mongoz*	Active quadrupedalism	4	3	3.18
	Hapalemur griseus	Vertical clinging and leaping	6	2	2.54
	Lemur catta	Active quadrupedalism	5	3	3.18
	Varecia variegata	Active quadrupedalism	5	3	3.18
Lorisidae	*Loris tardigradus*	Slow-climbing quadrupedalism	3	2	1.27
	Nycticebus pygmaeus	Slow-climbing quadrupedalism	3	3	1.27

specimens used in the analyses). Bones were digitized using a Breuckmann 3D surface scanner at the MNHN, Paris. This surface scanner allows the acquisition of 3D surface of the bone using white light fringes (StereoSCAN^{3D} model with a camera resolution of 5 megapixels).

2.1.1 | Subjects and kinetic data collection

In addition, data on peak vertical forces were collected for the same species (Table 1). Adult individuals of *Loris tardigradus*, *Nycticebus pygmaeus*, *Eulemur mongoz*, *Daubentonia madagascariensis*, *Propithecus coquereli*, *Hapalemur griseus*, *Lemur catta*, and *Varecia variegata* were used in this study (Table 1). All data were gathered from animals housed at the Duke Lemur Center (Durham, NC).

All procedures were approved by the appropriate institutional IACUCs (Duke: A104-09-03; A130-07-05, A270-11-10). The data collection procedures have been described extensively elsewhere (Demes et al., 1994; Granatosky, Tripp, & Schmitt, 2016a; Schmitt & Hanna, 2004; Schmitt & Lemelin, 2002; Schmitt & Lemelin, 2004) and will be simply summarized here. Subjects were encouraged by a food reward to walk on a pole raised above and firmly attached to the floor of the enclosure. The pole varied in diameter between 1.27 and 3.18 cm (Table 1) and was at least 4 m long. Pole diameters were chosen on the basis of previously published studies (Granatosky, Tripp, & Schmitt, 2016a; Hanna, Granatosky, Rana, & Schmitt, 2017), which generally attempt to use the smallest pole the animals will utilize (Schmitt & Hanna, 2004). A short middle section of the pole, wide enough for a single hand contact, was instrumented with a force transducer (MC3A-6®; AMTI, Watertown, MA), or force transducers (9317B; Kistler, Amherst, NY), following Schmitt and Hanna (2004) and Granatosky, Tripp, and Schmitt (2016a), which recorded ground reaction forces in three orthogonal directions. As the animals moved across the pole, they were video recorded using cameras (A602f; Basler AG, Ahrensburg, Germany, Sony Handycam, or GoPro Hero3+) at 60–120 frames per second [see Granatosky, Tripp, Fabre, & Schmitt, 2016b for information on data collection with GoPro cameras]. Only trials in which the animal was traveling in a straight path and not accelerating or decelerating (i.e., steady-state locomotion) throughout the walking trial, in which a full forelimb contacted the instrumented pole, and which exhibited a symmetric footfall sequence were retained for analysis. From these data, five variables were calculated for each limb: (1) vertical peak force; (2) propulsive peak force; (3) braking peak force; (4) medially directed peak force; and (5) laterally directed peak force (Supporting Information Table S2). For all data, steady-state locomotion was determined by a combination of video-recording and force traces following the methods of Granatosky, Tripp, and Schmitt (2016a; Granatosky, Tripp, Fabre, et al., 2016b), Schmitt and Lemelin (2002) and Schmitt and Hanna (2004). For all trials, symmetry was determined using the methods of Cartmill, Lemelin, and Schmitt (2002), with a ± 10 criterion such that the timing of opposite limb touchdown could vary between 40 and 60% of the stride cycle (50% indicates the timing of opposing limbs is exactly 1/2 of the cycle).

2.1.2 | Data processing for kinetic data

Force data were converted from raw voltage data to Newtons for each transducer. The force transducers were calibrated daily using a known mass before or after data collection. Forces were then filtered using a low-pass, 2-way Butterworth or Fourier filter with a 60 Hz cutoff. Cameras were calibrated for distance using a known length in the view of the camera in the same plane as the animal was moving. Speed was determined from this calibration as the average velocity of the animal over the view of the camera, by the position of the head marker from the initial view in the cameras to the last view in the camera (Supporting Information Table S2). Contact time was determined as the time each hand or foot was in contact with the instrumented pole. For all analyses described below, we used the absolute value of each of the peak forces collected.

2.1.3 | Quantification of shape using 3D geometric morphometrics

The shape of each forelimb long bone is complex and cannot be accurately represented using a traditional landmark based approach (Fabre et al., 2013b; Fabre et al., 2015b; Fabre et al., 2017; Fabre, Cornette, Goswami, & Peigné, 2015a; Fabre, Cornette, Peigné, & Goswami, 2013a; Fabre, Goswami, Peigné, & Cornette, 2014). Consequently, a 3D sliding-semilandmark procedure (Bookstein, 1997; Gunz, Mitteroecker, & Bookstein, 2005) was used in addition to standard anatomical landmarks to quantify their morphology, and especially their articulations and diaphyses. Through this procedure, sliding-semilandmarks slide on surfaces and curves and are transformed into geometrically (i.e., spatially) homologous landmarks that can be used to compare shapes (Parr et al., 2012). Semilandmarks are allowed to slide along the curves and surfaces that are predefined while minimizing the bending energy. Anatomical landmarks and sliding-

semilandmark of curves were obtained from 3D surface scans of each bone using the software package Idav Landmark (Wiley et al., 2005), while the library "Morpho" (Schlager, 2013) in R (Hornik, 2015) was used to perform the sliding-semilandmark procedure. To do so, we first created a template for each long bone following the method of Cornette, Baylac, Souter, and Herrel (2013) with 27 anatomical landmarks, 99 sliding-semilandmarks on curves and 265 sliding-semilandmarks on surfaces for the humerus (Fabre et al., 2017); 25 anatomical landmarks, 97 sliding-semilandmarks on curves, and 311 sliding-semilandmarks on surfaces for the ulna (Fabre et al., 2017); 21 anatomical landmarks, 49 sliding-semilandmarks on curves, and 252 sliding-semilandmarks on surfaces for the radius (Fabre et al., 2017). Based on the homologous landmarks and curves taken on the specimen, all the sliding-semilandmarks (curve and surface sliding-semilandmarks) of the template are projected onto the new specimen using a thin plate spline deformation (Gunz & Mitteroecker, 2013). All these steps were performed using the library "Morpho" (Schlager, 2013) that follows the algorithm of Gunz et al. (2005), which is implemented in R (Hornik, 2015). After projection four thin-plate spline relaxations were performed, the first relaxation was performed against the template, and the three others against Procrustes consensus calculated using the data from the previous iteration. Both sliding and relaxation are repeated iteratively until the bending energy is minimized (Schlager, 2013). After this operation has been performed, the landmarks of all specimens can be compared using traditional geometric morphometric methods.

Once all landmark data were obtained, a generalized Procrustes superimposition (Rohlf & Slice, 1990) was performed using the library "Geomorph" (Adams & Otarola-Castillo, 2013) in R (Hornik, 2015). Finally, a mean shape was calculated for each species using the Procrustes coordinates. This mean shape was then used in all subsequent analyses.

2.1.4 | Methods for analysis of the effect of body mass on bone shape and peak forces

In order to assess the effect of the body mass on the shape of the forelimb as well as on the peak forces, a regression of the log10-transformed body mass on the shape of the forelimb, as well as on the peak forces was performed. To do so, the "ProcD.lm" function of the "Geomorph" (Adams & Otarola-Castillo, 2013) library in R (Hornik, 2015) was used. Next, Procrustes coordinates (body mass free-shape) as well as peak forces (residuals of the peak forces) of each species were obtained. The body mass of each animal was obtained just before each trial. A mean body mass was calculated per species. For this study, we decided to use the in vivo body masses because they are highly correlated with the size of the bones of the museum specimens (see Supporting Information document S3 for further analyses documenting correlations between body mass estimates from different sources). In addition, we also explore linear measures taken on the specimens used for the in vivo study as an alternative estimate of size. Most correlations are significant and overall, we obtain similar results using both types of body mass estimates suggesting that this analysis is robust (see the results in Supporting Information document S3).

2.1.5 | Methods for correlation between velocity and peak forces

Because the speed of locomotion can also affect the peak forces (Demes et al., 1994), we tested for correlations between locomotor velocity and the substrate reaction forces using the "cor.test" function in R (Hornik, 2015).

2.1.6 | Methods for analysis of covariance

A traditional analysis of covariance (ANCOVA) using Type III sums of squares with log10-transformed body mass as a covariate was used to test whether species with different locomotor behaviors differ in the pattern of locomotor forces independent of variation in body mass. We defined three categories of locomotor behaviors following Anemone's (1993) and Gebo's (1993) definitions: active arboreal quadrupedalism, slow-climbing quadrupedalism, and vertical clinging and leaping (Table 1). When the co-variate was not significant, we performed a traditional analysis of variance (ANOVA) on peak forces with associated post hoc test to determine if species with different locomotor behaviors differ from another in loading regime. A Bonferroni correction was applied to the post-hoc tests to correct for multiple testing. All the analyses were performed in R (Hornik, 2015).

2.1.7 | Methods for assessing the effect of phylogeny on bone shape and peak forces

The phylogenetic tree of strepsirrhines used in our analyses is based on Herrera and Dávalos (2016). This is a time-calibrated maximum clade credibility phylogeny (Herrera & Dávalos, 2016). It uses 421 morphological, 5,767 protein-coding molecular characters as a backbone. Full details of the phylogenetic reconstruction and the tree are provided in Herrera and Dávalos (2016). This tree was pruned to include only the species included in our analysis and used in all subsequent comparative analyses with branch lengths proportional to geological time.

To estimate the phylogenetic signal a univariate Pagel's λ (1999) was calculated for each peak force, the log10 of body mass, and on the first three principal component (PC) axes (accounting for more than 90% of the overall variance: humerus: PC1 = 69.30%, PC2 = 15%, PC3 = 6.91%; ulna: PC1 = 72.39%, PC2 = 12.35%, PC3 = 9.83%; radius: PC1 = 63.15%, PC2 = 22.53%, PC3 = 5.25%) for each long bone of the forelimb using the function "phylosig" in the "phytools" library (Revell, 2012) in R (Hornik, 2015).

2.1.8 | Methods for analysis of covariation between forelimb shape and peak forces using two-block partial least squares

To quantify co-variation between each of the long bones of the forelimb and the peak forces used by animals during locomotion, we used 2B-PLS approaches (Rohlf & Corti, 2000) implemented in the library Geomorph (Adams & Otarola-Castillo, 2013) in R (Hornik, 2015). This method allows us to study co-variation between peak forces and the shape of each bone of the forelimb. In this method a covariance matrix is calculated from two blocks representing the variation of the two objects (peak forces—humerus shape, peak forces—ulna shape, and peak forces—radius shape). Two-block partial least square

analyses allow exploration of the patterns of covariation by a reduction of dimensionality of the data, generating axes that explain the covariance between the shape and the peak forces. Compared to a PCA, a PLS yields axes that are ordered from the pair that explains the maximum of covariance to the minimum of covariance for each pair of block, and each set of axes are orthogonal (Zelditch, Swiderski, & Sheets, 2012). Principal component analysis differs from 2B-PLS by the fact that the first examines the variance within a block whereas the second examines the covariance between two blocks. Two-block partial least squares analysis employs a mathematical technique called "Singular Value Decomposition" (SVD) which is a decomposition by eigenanalysis (eigen-decomposition) that extracts principal components from the variance–covariance matrix and partial warps (or vectors) from the bending-energy matrix (Zelditch et al., 2012). Thus, patterns of covariance between two blocks can be explored and PLS axes can be plotted, helping us to understand the co-variation between the peak forces and the shape of each long bones of the forelimb. Finally, a PLS coefficient of correlation between the two blocks of the PLS scores (r_{PLS}) is calculated allowing to estimate the degree of co-variation between the shape of the long bones and peak forces. The singular values were calculated by singular value decomposition of the covariance matrix following Rohlf and Corti (2000). PLS coefficient significance is calculated by comparing the singular value decomposition of the common covariance block to those obtained from permuted blocks. In the current study, the PLS coefficient was calculated using the function "pls2b" in R (Hornik, 2015) using the "Morpho" library (Schlager, 2013) following the method PLS (Bookstein et al., 2003). This function uses 3D landmark data after superimposition and performs an analysis which is referred to as singular warps analysis (Bookstein et al., 2003). A significance test is obtained by 1,000 permutations of the landmarks in one block relative to those of the first log10-transfromed of the peak forces in the other. Then a sampling distribution of coefficients is obtained by resampling. The p_{95} value is calculated by comparison of the observed PLS coefficient to those obtained after resampling. The significance of each linear combination is assessed by comparing the singular value (PLS coefficient) to those obtained from permuted blocks. If the PLS coefficient is higher than those obtained from permutated blocks, then its associated p_{95} value is considered as significant.

Because species share part of their evolutionary history, they cannot be treated as independent data points. Thus, we also conducted all analyses in a phylogenetic framework (Felsenstein, 1985; Harvey & Pagel, 1991) using the phylogeny described above. We use the "phylo.integration" function (Adams & Felice, 2014) in R using the Geomorph library (Adams & Otarola-Castillo, 2013). This function allows quantification of the degree of co-variation between the mean long bone shape of each species and the peak forces while accounting for phylogeny using a partial generalized least squares algorithm under a Brownian motion model of evolution (Adams & Felice, 2014). A matrix of evolutionary covariance is obtained, on which the "SVD" (singular value decomposition) is performed. It consists of the eigen-decomposition of this phylogenetic covariance matrix. From this step evolutionary PLS scores are calculated from the two blocks of phylogenetically corrected data and the evolutionary correlation between the two blocks of the PLS scores (r_{PLS}) is evaluated. PLS correlation significance is assessed using phylogenetic permutation, where the shape or the peak force values for all species for one block are permutated on the tips of the phylogeny. The derived correlation scores are obtained from the permutated datasets and can be compared to the observed value.

2.1.9 | Shape visualization at each extreme of the 2B-PLS and phylogenetic 2B-PLS axes

Shape visualization of the effect of peak forces on each long bones of the forelimb was performed using the "plsEffects," "warp. mesh," and "shade3d" functions of the "rgl" (Adler & Murdoch, 2012) and "Morpho" (Schlager, 2013) libraries functions in R (Hornik, 2015) and involved a thin-plate spline deformation of the 3D-scanned long bones of a *Lemur catta*. This function allows visualization of the shape at each extreme of the 2B-PLS axis, and thus to evaluate the kind of shape associated with the peak forces.

2.1.10 | Analysis of the influence of peak forces on forelimb shape

To test the effect of each peak force on the shape of each long bone separately (humerus, radius, and ulna), a regression was performed using "procD.lm" function in the geomorph library (Adams & Otarola-Castillo, 2013) in R (Hornik, 2015). To test the impact of each peak force on the shape of each bone separately, taking into account body mass, a regression was performed on the body mass free residuals of shape and peak forces. Finally, these analyses were performed in a phylogenetic framework to take into account the effect of the phylogeny, using the generalized partial least square (PGLS) method. A generalized partial least square was performed to test the effect of each peak force (and also the residuals) on the shape of each long bone (and residuals) separately while taking into account the phylogeny using the "procD.*pgls*" function of the "geomorph" library in R (Hornik, 2015).

3 | RESULTS

3.1 | Correlation between peak forces and locomotor velocity

No correlation was found between velocity and the vertical (t = 1.16, p = .28), fore-aft (braking: t = 0.63, p = .54; propulsive; t = 2.08, p = .08) or mediolateral peak forces (medially directed: t = 1.2, p = .24; laterally directed: t = 1.6, p = .16).

3.2 | Differences in peak forces between species with different locomotor behaviors

Body mass was a significant covariate for the braking, medially directed, and vertical peak forces (braking: $F_{1,4}$ = 12.84, p = .03; propulsive: $F_{1,4}$ = 0.15, p = .7; medially directed: $F_{1,4}$ = 16.7, p = .01; laterally directed: $F_{1,4}$ = 6.8, p = .06; vertical: $F_{1,4}$ = 114.8, p = .0004). An analysis of covariance was performed on the braking, medially directed, and vertical peak forces and showed that species with different habitual locomotor behaviors do not differ in peak forces (braking:

$F_{2,4}$ = 0.27, p = .78; medially directed: $F_{2,4}$ = .066, p = .94; vertical: $F_{2,4}$ = 2.19, p = .23). ANOVAs and associated post-hoc tests were performed on the propulsive and laterally directed peak forces given that the co-variate (body mass in this case) was not significant. These tests showed that laterally directed peak force does not differ depending on locomotion mode. However, propulsive peak forces differ depending on habitual locomotor behaviors ($F_{2,5}$ = 16.45, p = .006). Post-hoc tests show this difference is significant between active arboreal quadrupeds (relatively high propulsive peak forces) and slow quadrupedal species (relatively low propulsive forces) (p = .007, significant after Bonferroni correction).

3.3 | Phylogenetic signal

There is a significant phylogenetic signal in the first principal component (PC) axis describing the shape of each long bone of the forelimb (humerus PC1: Pagel's λ = 0.99, p = .047) in the third PC describing the shape of the ulna (ulna PC3: Pagel's λ = 0.99, p = .04) and in the second PC describing the shape of the radius (radius PC2: Pagel's λ = 0.99, p = .01). Otherwise, there is no phylogenetic signal in any of the other PCs describing the shape of each long bone of the forelimb (humerus PC2: Pagel's λ = 0.99, p = .26; humerus PC3: Pagel's λ = .00006, p = 1; ulna PC1: Pagel's λ = 0.99, p = .08; ulna PC2: Pagel's λ = .00006, p = 1; radius PC1: Pagel's λ = 0.99, p = .30; radius PC3: Pagel's λ = .00006, p = 1). The results are also not significant for the peak forces (braking: Pagel's λ = 0.85, p = .19; propulsive: Pagel's λ = 0.99, p = .06; medially directed: Pagel's λ = 0.99, p = .051; laterally directed: Pagel's λ = 0.99, p = .15; vertical: Pagel's λ = 0.99, p = .1). But there is a tendency for significant phylogenetic signal in body mass (Pagel's λ = 0.99, p = .052). Note, however, that our data set is small and that previous analyses incorporating a larger sample of species did find a significant phylogenetic signal (Fabre et al., 2017).

3.4 | Effect of body mass on the peak forces and the shape of the long bones of the forelimb

Body mass impacts all the peak forces (braking: R^2 = 0.920, p = .001; propulsive: R^2 = 0.570, p = .018; laterally directed: R^2 = 0.860, p = .002; medially directed: R^2 = 0.950, p = .001; vertical: R^2 = 0.970, p = .001; Table 2). These results are still significant even when accounting for phylogeny for the vertical peak force (R^2 = 0.955, p = .001; Table 2), for the braking peak force (R^2 = 0.770, p = .001; Table 2), and for the mediolateral peak forces (laterally directed: R^2 = 0.603, p = .011; medially directed: R^2 = 0.770, p = .004; Table 2). However, the results for the propulsive peak force are not significant anymore when accounting for phylogeny (propulsive: R^2 = 0.220, p = .172; Table 2). The results of the regressions of the $\log_{10}$ body mass on the shape of the long bones are significant for the humerus and the radius (Humerus: R^2 = 0.54, p = .009; Ulna: R^2 = 0.490, p = .011; Radius: R^2 = 0.4, p = .03; Table 3). These results are not significant when the phylogeny is taken into account (Humerus: R^2 = 0.240, p = .084; Ulna: R^2 = 0.260, p = .086; Radius: R^2 = 0.220, p = .081; Table 3).

TABLE 2 Results of the regression analyses testing for the effect of the log10 of body mass on the log10 of peak forces

	Regression		Phylogenetic regression	
Peak force	R^2	p Value	R^2	p Value
X braking	**0.920**	**.001**	**0.770**	**.001**
X propulsive	**0.570**	**.018**	0.220	0.172
Y lateral	**0.860**	**.002**	**0.603**	**.011**
Y medial	**0.950**	**.001**	**0.770**	**.004**
Z vertical	**0.970**	**.001**	**0.955**	**.001**

TABLE 3 Results of the regression analysis testing the effect of the log10 of body mass on the shape of each long bone of the forelimb

	Regression		Phylogenetic regression	
Bone	R^2	p Value	R^2	p Value
Humerus	**0.540**	**.009**	0.240	.084
Ulna	**0.490**	**.011**	0.260	.086
Radius	**0.400**	**.030**	0.220	.081

Significant results are indicated in bold.

3.5 | Regression analysis testing the associations of peak forces on the shape of each long bone of the forelimb

3.5.1 | Association of each peak force on the shape of the long bones of the forelimb

The results of the regression analyses testing the effect of the peak forces on the shape of each long bone of the forelimb are all significant (Table 4). When accounting for the influence of phylogeny, only the propulsive and medially directed peak forces impact the shape of the humerus; the propulsive, medially directed, and laterally directed peak forces also impact the shape of the ulna and the radius (Table 4).

3.5.2 | Associations of the residuals of the peak forces on the residuals of the shape of each long bone of the forelimb

The results of the regression analysis testing the impact of the residuals of the peak forces on the residuals of shape, as a method to control the effect of body size, are only significant for the propulsive force and the humerus (Table 4). When accounting for the influence of phylogeny, the propulsive force impacts the shape of both the humerus and the ulna (Table 4).

3.6 | Co-variation between each long bone of the forelimb and peak forces

3.6.1 | Humeral shape and peak forces

There is strong co-variation between the humeral shape and aspects of the peak forces even when body mass is taken into account (Figure 1, Table 5). However, the co-variation is not significant anymore when the phylogeny is taken into account (Table 5). The scatterplot of the traditional 2B-PLS (Figure 1a) differentiates slow-climbing quadrupedal lorises (*Loris* and *Nycticebus* along the negative part of the axis) from active arboreal quadrupeds (*Varecia*, *Daubentonia* and *Eulemur* along the positive part of the axis) and vertical clinger leapers (*Hapalemur* and *Propithecus* along the positive part of the axis). Slow-climbing quadrupedal species display a low fore-aft peak force

TABLE 4 Results of the regression analysis testing the effect of the log10 of the peak forces (*X*, *Y*, and *Z*) on the shape of each long bone of the forelimb

		Regression		Phylogenetic regression		Regression on residuals		Phylogenetic regression on residuals	
Bone	Peak force	R^2	*p* Value	R^2	*p* Value	R^2	*p* Value	R^2	*p* Value
Humerus	X braking	**0.460**	**.018**	0.100	0.400	0.110	0.580	0.162	0.621
	X propulsive	**0.621**	**.002**	**0.411**	**.001**	**0.390**	**.003**	**0.362**	**.013**
	Y medial	**0.540**	**.004**	**0.300**	**.012**	0.130	0.410	0.175	0.770
	Y lateral	**0.484**	**.007**	0.243	.103	.087	0.730	0.109	0.862
	Z vertical	**0.525**	**.011**	0.258	.084	0.118	0.545	.080	0.845
Ulna	X braking	**0.450**	**.022**	0.180	0.290	.020	0.970	.035	0.970
	X propulsive	**0.560**	**.004**	**0.470**	**.001**	0.360	.060	**0.390**	**.040**
	Y medial	**0.530**	**.005**	**0.380**	**.003**	0.180	0.250	0.260	0.340
	Y lateral	**0.530**	**.008**	**0.390**	**.014**	0.170	0.290	0.240	0.300
	Z vertical	**0.510**	**.011**	0.310	.060	0.130	0.430	0.130	0.480
Radius	X braking	**0.340**	**.038**	0.130	0.420	.054	0.820	.085	0.800
	X propulsive	**0.466**	**.010**	**0.416**	**.001**	0.216	0.201	0.290	0.110
	Y medial	**0.420**	**.016**	**0.320**	**.003**	0.150	0.283	0.230	0.390
	Y lateral	**0.400**	**.015**	**0.300**	**.030**	0.110	0.420	0.190	0.398
	Z vertical	**0.410**	**.024**	0.260	.053	0.130	0.380	0.140	0.410

associated with a relatively gracile, straight, and elongated humerus with a lateral crest that is not well developed, a distal articulation with a wide and round capitulum in comparison to the trochlea that is narrow and deep, and a humeral head that is oriented proximally (Figure 1a). In contrast, active arboreal quadrupeds and vertical clinger and leapers display a high fore-aft peak force (with a higher braking than propulsive force), a moderately high vertical peak force and, a high medially directed peak force and a relatively low laterally directed peak force that are associated with a relatively robust, curved and short humerus with a well-developed lateral crest, a distal articulation with a small capitulum in comparison to the trochlea that is elongated and shallow, and a humeral head that is oriented medially (Figure 1a).

In addition, when the effect of body mass is taken into account (Figure 1b) the larger vertical clinger and leaper (*Propithecus*) and the smaller slow-climbing quadrupedal loris (*Loris*) are positioned together along the negative side of the axis while the active arboreal quadrupedal lemurs (*Eulemur*, *Varecia*, *Daubentonia*, *Lemur*), the small vertical clinger and leaper (*Hapalemur*) and the big slow-climbing quadrupedal species (*Nycticebus*) are positioned toward the positive side of the axis. Species at the negative side of the axis display a medium braking peak force and relatively low other peak forces associated with a humeral shape that is relatively gracile, with a lateral crest that runs until one third of the length of the diaphysis, a distal articulation with a wide and round capitulum in comparison to a narrow trochlea. In opposition, species at the positive part of the axis display high propulsive peak force associated with a humeral shape that is relatively robust, a lateral crest that runs about midway the diaphysis, and a distal articulation with a small capitulum in comparison to the trochlea that is elongated (Figure 1b).

3.6.2 | Ulnar shape and peak forces

There is co-variation between the ulnar shape and peak forces (Figure 2 and Table 5). However, there is no co-variation when body mass and phylogeny are taken into account (Table 5).

The scatterplot of the traditional 2B-PLS between the ulnar shape and peak forces (Figure 2) is similar to the previous analysis of peak forces (Figures 1 and 2) and tends to differentiate the slow-climbing quadrupedal lorises at the negative side from the active arboreal quadrupeds and vertical clinger and leapers at the positive side. Slow-climbing quadrupedal species display lower than expected peak forces in association with a relatively gracile and antero-posteriorly curved ulna, with a short olecranon, a narrow proximal articulation, a distal radial notch that is ventrally oriented and a small styloid process (Figure 2). In contrast, active arboreal quadrupeds show high fore-aft and vertical peak forces associated with a relatively robust and medio-laterally curved ulna with an elongated olecranon, a wide proximal articulation, a medially well-developed lateral interosseous crest, a distal radial notch that is anteriorly oriented, and a wide styloid process (Figure 2).

3.6.3 | Radial shape and peak forces

Strong co-variation was observed between the radial shape and peak forces (Figure 3 and Table 5). Nevertheless, there is no co-variation when accounting for phylogeny and body mass (Table 5).

The scatterplot of the traditional 2B-PLS (Figure 3) differentiates, as it did for the humerus and ulna, active arboreal quadrupeds at the negative side of the axis from the slow-climbing quadrupedal lorises at the positive side. Active arboreal quadrupeds and vertical clinger and leapers species show a high braking and medially directed peak forces and rather high propulsive, laterally directed and vertical forces. These forces are associated with a relatively robust and medio-laterally curved radius, with a wide proximal articulation with a narrow lip, a distal radial notch that is anteriorly oriented, and a prominent styloid process (Figure 3). In contrast, slow-climbing quadrupedal species display low peak forces in association with a relatively gracile and antero-posteriorly curved radius, with a narrow proximal articulation with a wide lip, a distal radial notch that is dorsally oriented, and a small styloid process (Figure 3).

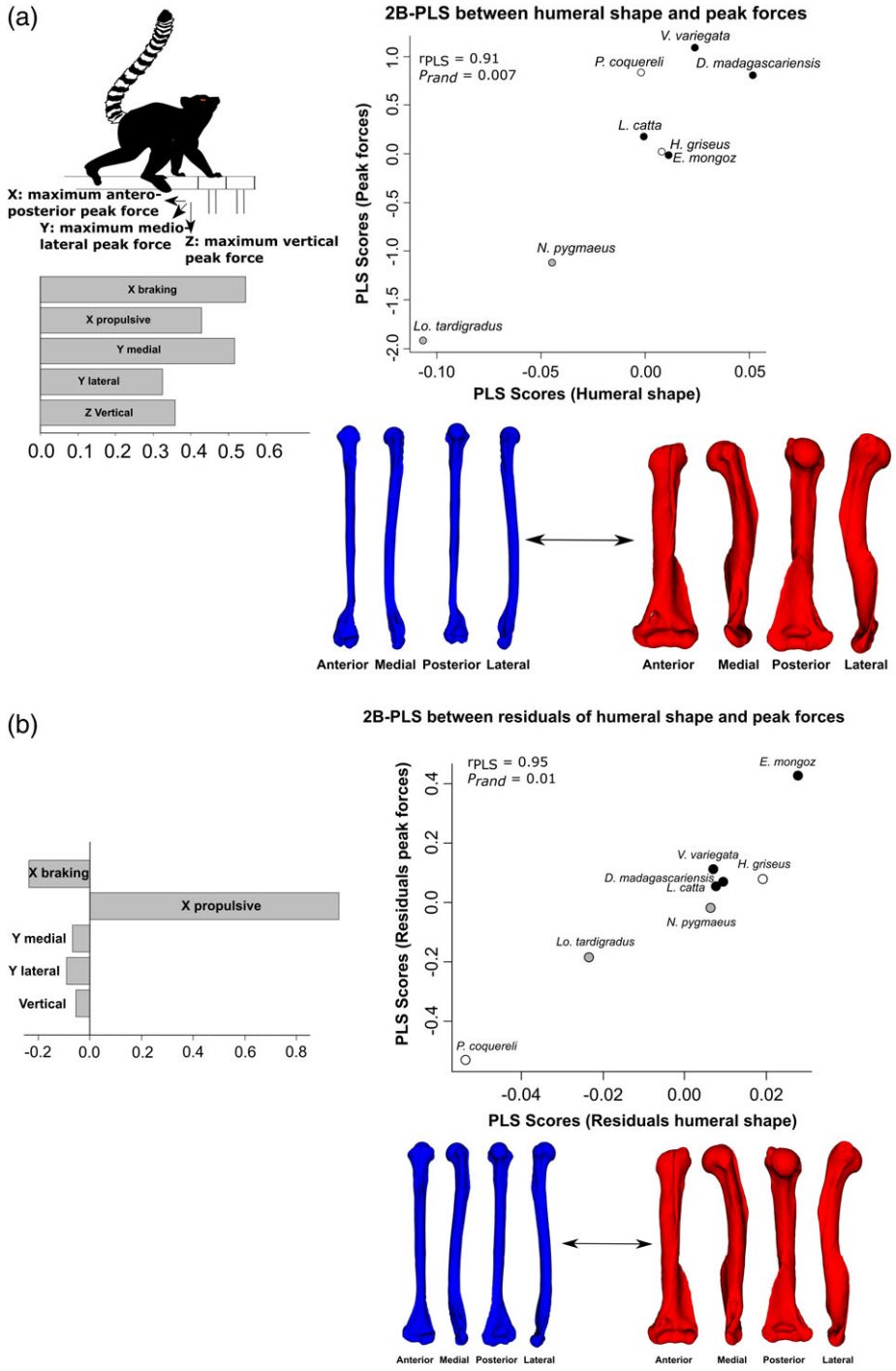

FIGURE 1 Results of the two-block partial least-squares between the humerus and the peak forces. (a) Scatter plot of the first partial least-squares axis describing the shape co-variation between the humerus and the peak forces. (b) Scatter plot of the first partial least-squares axis describing the shape co-variation between the residuals of the humerus and the residuals of the peak forces. Humeral shapes (left side) associated with each minimum and maximum of co-variation are illustrated in blue and red, respectively, at the bottom of the scatter plot. Peak force loadings associated with the humeral shape co-variation are represented by the histogram at the left side of the scatterplot. Symbols represent locomotor behaviors as follows: White circle indicating vertical clinging and leaping; gray circle indicating slow climbing; black circle indicating active quadrupedalism [Color figure can be viewed at wileyonlinelibrary.com]

4 | DISCUSSION

The question of to what extent bone shape is related to habitual locomotor behavior and to specific peak forces is long-standing and has profound impact on understanding form-function relationships and inferences of behavior in fossil taxa. For the most part the relationship between bone form and peak forces is presumed from ideas about loading and habitual locomotor behaviors and more detailed data are needed to explore these ideas. This study examined the influence of peak forces on forelimb long bone shape in the context of body size, phylogeny, and habitual locomotor mode in a novel and comprehensive sample of strepsirrhine primates in order to test hypotheses

TABLE 5 Results of the co-variation between the peak forces and the shape of each long bone of the forelimb and their residuals

	2B-PLS		Phylogenetic 2B-PLS		2B-PLS on residuals		Phylogenetic 2B-PLS on residuals	
Bone	r_{PLS}	*p* Value	r_{PLS}	*p* Value	r_{PLS}	*p* Value	r_{PLS}	*p* Value
HUMERUS	**0.910**	**.007**	0.790	0.200	**0.950**	**.010**	0.890	0.13
ULNA	**0.890**	**.009**	0.820	.07	0.840	0.150	0.860	0.160
RADIUS	**0.880**	**.010**	0.760	0.170	0.690	0.490	0.790	0.200

Significant co-variations are indicated in bold.

about form and function in primates. The findings showed a clear signal for the effect of peak forces and habitual locomotor mode on forelimb shape irrespective of phylogeny.

4.1 | Effect of phylogeny

The shape of the long bones of the forelimb showed a phylogenetic signal meaning that species that are closely related tend to show similar shapes. Otherwise, no phylogenetic signal was found for the peak forces during locomotion, at least for species included in our study. Nevertheless, the dataset included here is small and we suggest that these results should be interpreted cautiously. The addition of more species in the morphological data set will likely result in a stronger and/ or significant phylogenetic signal in limb bone shape and body mass as demonstrated previously (Fabre et al., 2017).

4.2 | Effects of body mass on peak forces

Body mass impacts the shape of the long bones, but this effect disappears when accounting for the shared history of species. It also strongly impacted the peak forces during locomotion even when taking into account the phylogeny (except for the propulsive force). More precisely, body mass has a strong impact on the vertical peak force as

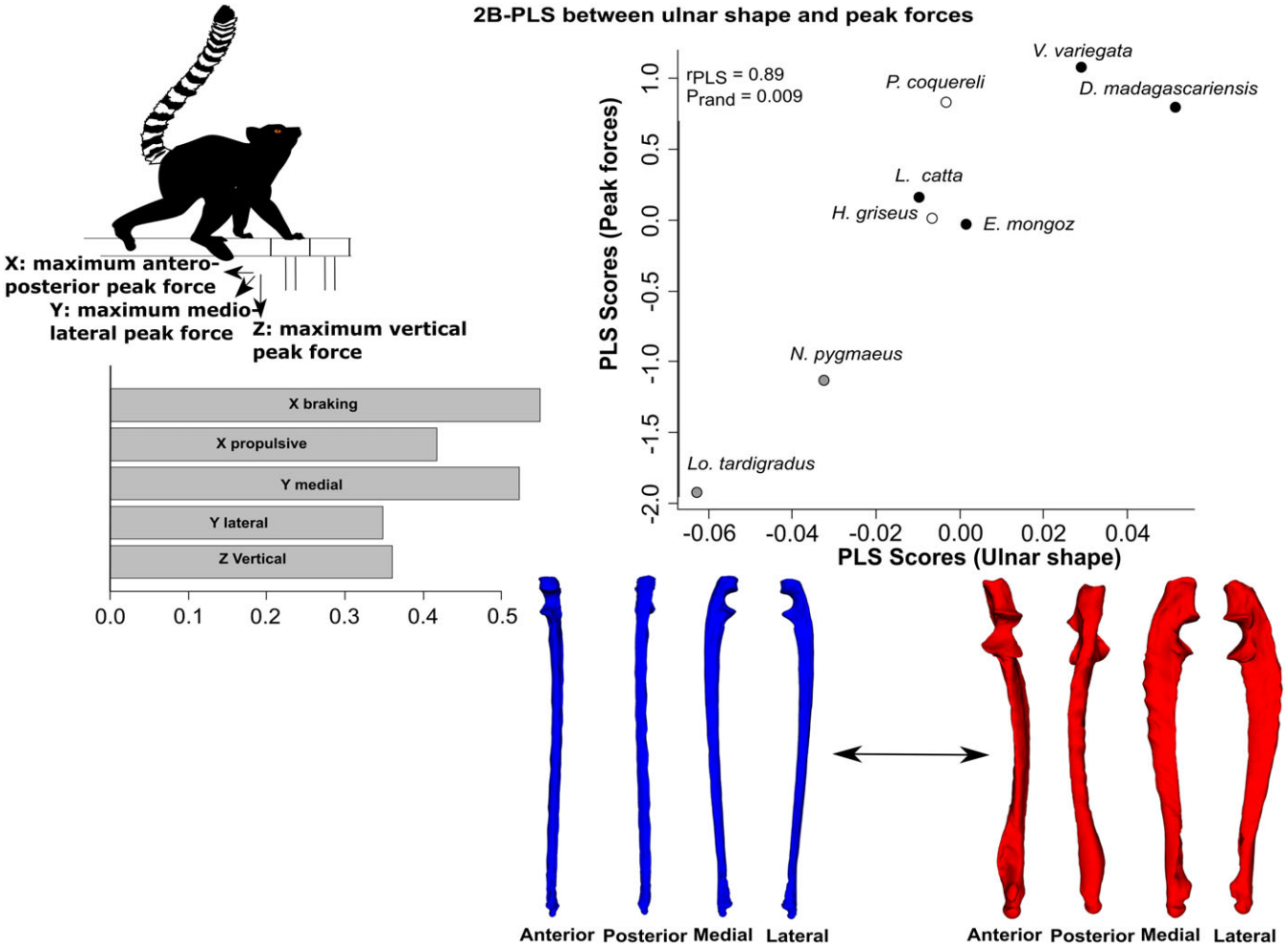

FIGURE 2 Results of the two-block partial least-squares between the ulna and the loading regimes. Scatter plot of the first partial least-squares axis describing the shape co-variation between the ulna and the loading regime. Ulnar shapes (left side) associated with each minimum and maximum of co-variation are illustrated in blue and red, respectively, at the bottom of the scatter plot. Peak force loadings associated with the ulnar shape co-variation are represented by the histogram at the left side of the scatterplot. Symbols represent locomotor behaviors as follows: white circle indicating vertical clinging and leaping; gray circle indicating slow climbing; black circle indicating active quadrupedalism [Color figure can be viewed at wileyonlinelibrary.com]

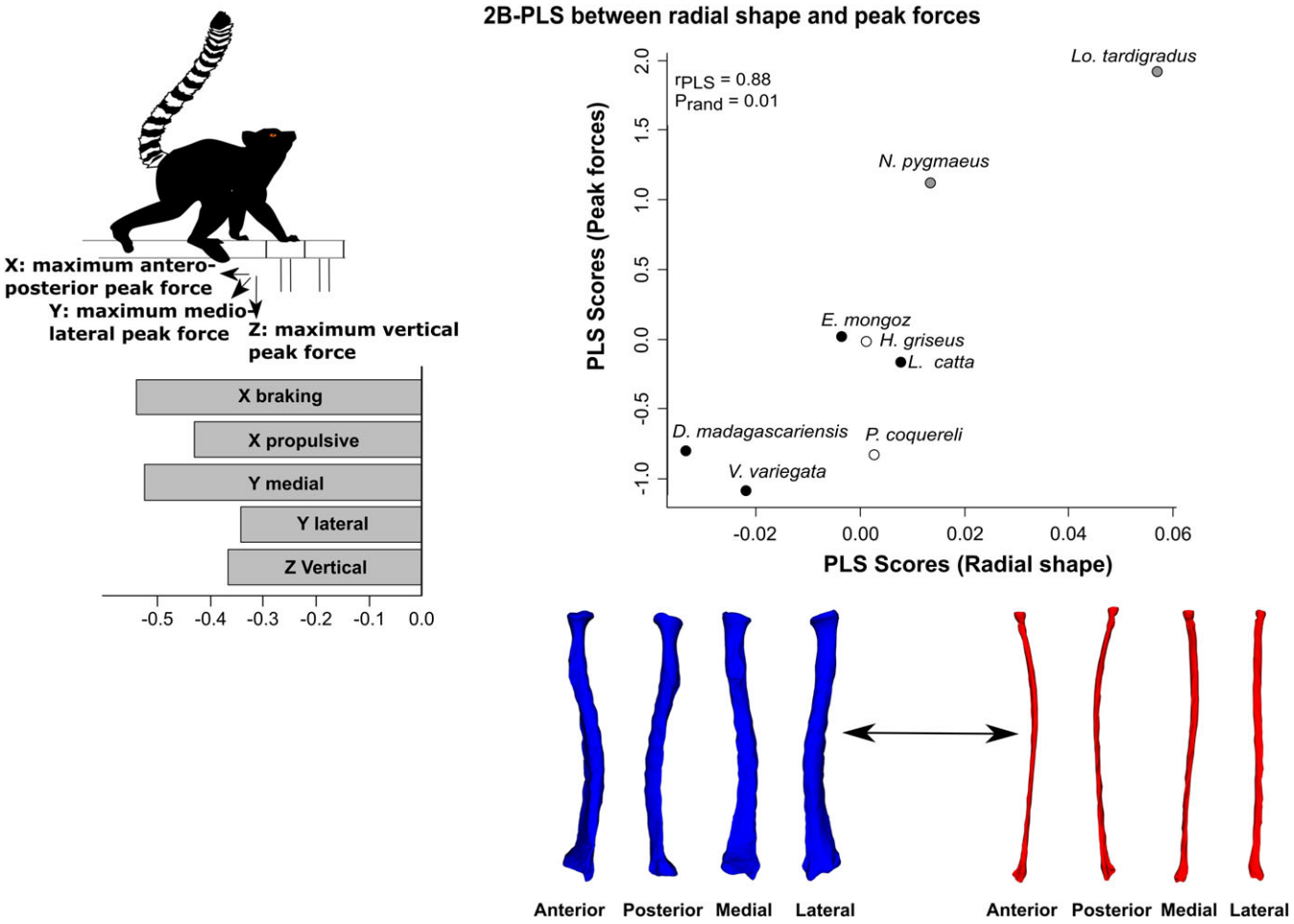

FIGURE 3 Results of the two-block partial least-squares between the radius and the loading regimes. Scatter plot of the first partial least-squares axis describing the shape co-variation between the radius and the loading regime. Radial shapes (left side) associated with each minimum and maximum of co-variation are illustrated in blue and red, respectively, at the bottom of the scatter plot. Peak force loadings associated with the radial shape co-variation are represented by the histogram at the left side of the scatterplot. Symbols represent locomotor behaviors as follows: white circle indicating vertical clinging and leaping; gray circle indicating slow climbing; black circle indicating active quadrupedalism [Color figure can be viewed at wileyonlinelibrary.com]

expected. It also strongly impacts the braking and medially directed peak forces.

4.3 | Effects of peak forces on bone shape

In the primary analysis, all the peak forces have an effect on the shape of the bones of the forelimb. However, when phylogeny is considered, only the propulsive and medially directed peak forces appear to impact the shape of the humerus. In addition, the propulsive and mediolateral peak forces have an effect on the shape of both the radius and ulna (Table 4). Contrary to expectations, the propulsive peak forces had the strongest effect on the shape of the humerus after accounting for the effect of body mass and phylogeny (Table 4). The propulsive peak force also strongly impacts the shape of the ulna when phylogeny and body mass are considered (Table 4). To summarize, contrary to our predictions, the effects of the propulsive peak force are mainly reflected in humeral and ulnar shapes. This suggests that humerus and ulna play an important role in absorbing, transferring, and dissipating propulsive forces during arboreal quadrupedal locomotion in strepsirrhines.

4.4 | Co-variation between peak forces and the shape of the forelimb

When looking at the co-variation between peak forces and the long bones of the forelimb, a common pattern becomes apparent. A clear difference can be seen between the slow-climbing quadrupedal species (such as the lorises) and the active arboreal quadrupeds (such as *Varecia*, *Daubentonia*, and *Eulemur*). For all three long bones of the forelimb, active arboreal quadrupeds with higher peak forces show robust bones with a curved shaft (medio-laterally for the humerus and antero-posteriorly for the ulna and radius), broad articulations, and well-developed crests. In contrast, slow quadrupedal species, which experience relatively low peak forces compared to other species show markedly more gracile bones and mobile articulations that appear to facilitate movements. These patterns are the most noticeable for the humerus and the radius. This is reflected in the arboreal/terrestrial differences described by Rose (1988) and Fabre et al. (2017).

When accounting for body mass, only the co-variation between the peak forces and the humeral shape is significant; a clear difference can be seen between both the larger vertical clinger and leaper (*Propithecus*), the smaller slow-climbing quadrupedal loris (*Loris*) and

the other species (*Nycticebus*, *Daubentonia*, *Eulemur*, *Lemur*, *Varecia*, *Hapalemur*). The force that co-varies most with humeral shape of the sifaka and the slender loris is a medium braking peak force and relatively lower other forces. The shapes associated with these forces show a relatively gracile bone, with a lateral crest that runs until one third of the length of the diaphysis, a distal articulation with a wide and round capitulum in comparison to a narrow trochlea. In opposition, all the other species display high propulsive peak force associated with a humeral shape that is relatively robust, a lateral crest that runs about midway the diaphysis, and a distal articulation with a small capitulum in comparison to the trochlea that is elongated. The strongest co-variation is observed between the peak forces and the humeral shape suggesting that this bone plays an important role in absorbing, transferring, and dissipating locomotor forces.

4.5 | Functional interpretations

The findings of this study have profound implications for reconstructing the movement patterns of extinct primates based on forelimb anatomy. First, it is clear that "primary locomotor mode" (e.g., active arboreal quadruped, or vertical clinger and leaper) tells us little about the way the forelimb might be shaped in strepsirrhines after accounting for phylogenetic or body-size differences. We implore future investigators to be wary of these broad locomotor classifications, and instead take a critical look at the ways these animals move on commonly used substrates.

Throughout all of our analyses, it has become obvious that the association between osseous morphology and external loading in the forelimb is driven primarily by propulsive forces. As recently demonstrated by Granatosky et al., (2018), propulsive forces of the forelimb appear to be higher in primates than other mammals.

To conclude, our study shows strong, significant co-variation between the shape of the long bones and the peak forces generated by the forelimb as measured by force plate recordings during arboreal quadrupedal locomotion. The propulsive and medially directed peak forces co-vary most strongly with the shape of the long bones of the forelimb. Thus, our results suggest that the shape of humerus and ulna significantly reflects how it is loaded suggesting that external locomotor forces play a role in driving the overall shape of long bones in the forelimb in strepsirrhines, although the direct relationship between load and bone anabolism remains unclear. Whether the ground reaction forces coming from quadrupedal walking on a pole are direct drivers of bone shape or indirectly related to bone shape through lifetime effects of locomotor specializations or whether these features are simply a product of natural selection for specific shapes remains to be tested. Irrespective, the associations described here between long bone shape and habitual locomotor behavior may provide critical insights when trying to interpret the bones of extinct taxa, thus, providing a window on their locomotor behavior and ecology.

ACKNOWLEDGMENTS

We thank Erin Ehmke, David Brewer, and Meg Dye at the Duke Lemur Center for all the help with animal training and data collection. We thank J. Cuisin, C. Bens, and A. Verguin for access to the specimens from the collections of Anatomie Comparée, MNHN, Paris. We thank A. Blin from the "plate-forme de morphométrie" of the UMS 2700 (CNRS, MNHN) for access to the surface scanner. This is Duke Lemur Center Publication Number #1404. The authors would like to thank two anonymous reviewers who made helpful and constructive suggestions that improved the manuscript.

ORCID

Anne-Claire Fabre http://orcid.org/0000-0001-7310-1775

REFERENCES

Adams, D. C., & Otarola-Castillo, E. (2013). Geomorph: An R package for the collection and analysis of geometric morphometric shape data. *Methods in Ecology and Evolution*, *4*, 393–399.

Adams, D. C., & Felice, R. (2014). Assessing phylogenetic morphological integration and trait covariation in morphometric data using evolutionary covariance matrices. *PLoS One*, *9*(4), e94335.

Adler, D., & Murdoch, D. (2012). *rgl: 3D visualization device system (OpenGL). R Package Version* (pp. 95–1201). Vienna, Austria: The R Foundation for Statistical Computing.

Alexander, R. M. N. (1980). Optimum walking techniques for quadrupeds and bipeds. *Journal of Zoology*, *173*, 549–573.

Alexander, R. M. N. (1996). *Optima for animals*. Princeton, NJ: Princeton University Press.

Allan, G. H., Cassey, P., Snelling, E. P., Maloney, S. K., & Seymour, R. S. (2014). Blood flow for bone remodeling correlates with locomotion in living and extinct birds. *Journal of Experimental Biology*, *217*, 2956–2962.

Anemone, R. L. (1993). The functional anatomy of the hip and thigh in Primates. In D. L. Gebo (Ed.), *Postcranial adaptation in nonhuman Primates* (pp. 150–174). DeKalb, IL: Northern Illinois University Press.

Arnold, S. J. (1983). Morphology, performance and fitness. *American Zoologist*, *23*, 347–361.

Bertram, J. E., & Biewener, A. A. (1988). Bone curvature: Sacrificing strength for load predictability? *Journal of Theoretical Biology*, *131*, 75–92.

Bertram, J. E. A., & Swartz, S. M. (1991). The 'law of bone transformation': A case pf crying Wolff? *Biological Reviews*, *66*, 245–273.

Biewener, A. A. (1982). Bone strength in small mammals and bipedal birds: Do safety factors change with body size. *Journal of Experimental Biology*, *98*, 289–301.

Biewener, A. A. (1983a). Locomotory stresses in the limb bones of two small mammals: The ground squirrel and chipmunk. *Journal of Experimental Biology*, *103*, 131–154.

Biewener, A. A. (1983b). Allometry of quadrupedal locomotion: The scaling of duty factor, bone curvature and limb orientation to body size. *Journal of Experimental Biology*, *105*, 147–171.

Biewener, A. A. (1989). Scaling body support in mammals: Limb posture and muscle mechanics. *Science*, *245*, 45–48.

Biewener, A. A. (1991). Musculoskeletal design in relation to body size. *Journal of Biomechanics*, *24*, 19–29.

Biewener, A. A. (2005). Biomechanical consequences of scaling. *Journal of Experimental Biology*, *208*, 1665–1676.

Blob, R. W., & Biewener, A. A. (2001). Mechanics of limb bone loading during terrestrial locomotion in the green iguana (*Iguana iguana*) and American alligator (*Alligator mississippiensis*). *Journal of Experimental Biology*, *204*, 1099–1122.

Bookstein, F. L. (1997). Landmark methods for forms without landmarks: Morphometrics of group differences in outline shape. *Medical Image Analysis*, *1*, 225–243.

Bookstein, F. L., Gunz, P., Mitteroecker, P., Prossinger, H., Schaefer, K., & Seidler, H. (2003). Cranial integration in Homo: Singular warps analysis of the midsagittal plane in ontogeny and evolution. *Journal of Human Evolution*, *44*, 167–187.

Budsberg, S. C., Verstraete, M. C., & Soutas-Little, R. W. (1987). Force plate analysis of the walking gait in healthy dogs. *American Journal of Veterinarian Research*, *48*, 915–918.

Burr, D. B. (2002). Targeted and nontargeted remodeling. *Bone*, *30*, 2–4.

Carlson, K. J., Demes, B., & Franz, T. M. (2005). Mediolateral forces associated with quadrupedal gaits of lemurids. *Journal of Zoology*, *266*, 261–273.

Cartmill, M., Lemelin, P., & Schmitt, D. (2002). Support polygons and symmetrical gaits in mammals. *Zoological Journal of the Linnean Society*, *136*, 401–420.

Cornette, R., Baylac, M., Souter, T., & Herrel, A. (2013). Does shape co-variation between the skull and the mandible have functional consequences? A 3D approach for a 3D problem. *Journal of Anatomy*, *223*, 329–336.

Currey, J. D. (2002). *Bones: Structure and mechanics*. Princeton, NJ: Princeton University Press.

Currey, J. D. (2003). The many adaptations of bone. *Journal of Biomechanics*, *36*, 1487–1495.

Demes, B., Larson, S. G., Stern, J. T., Jungers, W. L., Biknevicius, A. R., & Schmitt, D. (1994). The kinetics of primate quadrupedalism: "Hindlimb drive" reconsidered. *Journal of Human Evolution*, *26*, 353–374.

Demes, B., Stern, J. T., Hausman, M. R., Larson, S. G., McLeod, K. J., & Rubin, T. (1998). Patterns of strain in the macaque ulna during functional activity. *American Journal of Physical Anthropology*, *106*, 87–100.

Demes, B., Qin, Y. X., Stern, J. T., Larson, S. G., & Rubin, C. T. (2001). Patterns of strain in the macaque tibia during functional activity. *American Journal of Physical Anthropology*, *116*, 257–265.

Fabre, A.-C., Cornette, R., Peigné, S., & Goswami, A. (2013a). Influence of body mass on the shape of forelimb in musteloids carnivorans. *Biological Journal of the Linnean Society*, *110*, 91–103.

Fabre, A.-C., Cornette, R., Slater, G., Argot, C., Peigné, S., Goswami, A., & Pouydebat, E. (2013b). Getting a grip on the evolution of grasping in musteloid carnivorans: A three-dimensional analysis of forelimb shape. *Journal of Evolutionary Biology*, *26*, 1521–1535.

Fabre, A.-C., Goswami, A., Peigné, S., & Cornette, R. (2014). Morphological integration in the forelimb of musteloid carnivorans. *Journal of Anatomy*, *225*, 19–30.

Fabre, A.-C., Cornette, R., Goswami, A., & Peigné, S. (2015a). Do constraints associated with the locomotor habitat drive the evolution of forelimb shape? A case study in musteloid carnivorans. *Journal of Anatomy*, *226*, 596–610.

Fabre, A.-C., Salesa, M. J., Cornette, R., Antón, M., Morales, J., & Peigné, S. (2015b). Quantitative inferences on the locomotor behaviour of extinct species applied to *Simocyon batalleri* (Ailuridae, late Miocene, Spain). *Science of Nature*, *102*, 30.

Fabre, A.-C., Marigó, J., Granatosky, M. C., & Schmitt, D. (2017). Functional associations between support use and forelimb shape in strepsirrhines and their relevance to inferring locomotor behavior in early primates. *Journal of Human Evolution*, *108*, 11–30.

Felsenstein, J. (1985). Phylogenies and the comparative method. *American Naturalist*, *125*, 1–15.

Fleagle, J. G. (2013). *Primate adaptation and evolution* (3rd ed.). New York: Elsevier Academic Press.

Franz, T. M., Demes, B., & Carlson, K. J. (2005). Gait mechanics of lemurid primates on terrestrial and arboreal substrates. *Journal of Human Evolution*, *48*, 199–217.

Gebo, D. L. (1987). Locomotor diversity in prosimian primates. *American Journal of Primatology*, *13*, 271–281.

Gebo, D. L. (1993). Functional morphology of the foot in Primates. In D. L. Gebo (Ed.), *Postcranial adaptation in nonhuman Primates* (pp. 175–196). DeKalb, IL: Northern Illinois University Press.

Granatosky, M. C., & Fitzsimons, A. (2017). Is all quadrupedalism the same? Form-function relationships in behaviorally distinct Asian colobines. *Journal of Vietnamese Primatology*, *2*, 59–72.

Granatosky, M. C., Tripp, C. H., & Schmitt, D. (2016a). Gait kinetics of above and below branch quadrupedal locomotion in lemurid primates. *Journal of Experimental Biology A*, *219*, 53–63.

Granatosky, M. C., Tripp, C. H., Fabre, A.-C., & Schmitt, D. (2016b). Patterns of quadrupedal locomotion in a vertical clinging and leaping primate (*Propithecus coquereli*) with implications for understanding the functional demands of primate quadrupedal locomotion. *American Journal of Physical Anthropology*, *160*, 644–652.

Granatosky, M. C., Fitzsimons, A., Zeininger, A., Schmitt, D. (2018). Mechanisms for the functional differentiation of the propulsive and braking roles of the forelimbs and hindlimbs during quadrupedal walking in primates and felines. *Journal of Experimental Biology 221*, 1–11.

Gunz, P., & Mitteroecker, P. (2013). Semilandmarks: A method for quantifying curves and surfaces. *Hystrix*, *24*, 103–109.

Gunz, P., Mitteroecker, P., & Bookstein, F. L. (2005). Semilandmarks in three dimensions. In D. E. Slice (Ed.), *Modern morphometrics in physical anthropology* (pp. 73–98). Berlin, Germany: Springer.

Hanna, J. B., Granatosky, M. C., Rana, P., & Schmitt, D. (2017). The evolution of vertical climbing in primates: Evidence from reaction forces. *Journal of Experimental Biology*, *220*, 3039–3052.

Harvey, P. H., & Pagel, M. D. (1991). *The comparative method in evolutionary biology*. Oxford: University Press Oxford.

Herrera, J. P., & Dávalos, L. M. (2016). Phylogeny and divergence times of lemurs inferred with recent and ancient fossils in the tree. *Systematic Biology*, *65*, 772–791.

Hildebrand, M. (1967). Symmetrical gaits of primates. *American Journal of Physical Anthropology*, *26*, 119–130.

Hildebrand, M. (1985). Walking and running. In M. Hildebrand, D. M. Bramble, K. F. Liem, & D. B. Wake (Eds.), *Functional vertebrate morphology* (pp. 38–57). Cambridge: Harvard University Press.

Hornik, K. (2015). *The R FAQ*. Vienna, Austria: The R Foundation for Statistical Computing. Retrieved from https://CRAN.R-project.org/doc/FAQ/R-FAQ.html

Huiskes, R., & van Rietbergen, B. (2005). Biomechanics of bone. In V. C. Mow & R. Huiskes (Eds.), *Basic orthopaedic biomechanics and Mechano-biology* (3rd ed., pp. 123–179). New York, NY: Lippincott Williams & Wilkins.

Hunt, K. D., Cant, J. G. H., Gebo, D. L., Rose, M. D., Walker, S. E., & Youlatos, D. (1996). Standardized descriptions of primate locomotor and postural modes. *Primates*, *37*, 363–387.

Hylander, W. L., & Johnson, K. R. (1997). In *vivo* bone strain patterns in the zygomatic arch of macaques and the significance of these patterns for functional interpretations of craniodental form. *American Journal of Physical Anthropology*, *102*, 203–232.

Kivell, T. L., Schmitt, D., & Wunderlich, R. E. (2010). Hand and foot pressures in the aye-aye (Daubentonia madagascariensis) reveal novel biomechanical trade-offs required for walking on gracile digits. *Journal of Experimental Biology*, *213*, 1549–1557.

Kimura, T., Okada, M., & Ishida, H. (1979). Kinesiological characteristics of primate walking: Its significance in human walking. In M. Morbeck, H. Preuschoft, & N. Gomberg (Eds.), *Environment, behaviour, morphology: Dynamic interactions in primates* (pp. 297–311). New York, NY: Gustav Fischer.

Krakauer, E., Lemelin, P., & Schmitt, D. (2002). Hand and body position during locomotor behavior in the aye-aye (Daubentonia madagascariensis). *Am J Primatol* 57, 105–118.

Lanyon, L. E., & Rubin, C. T. (1985). Functional adaptation in skeletal structures. In M. Hildebrand, D. M. Bramble, K. F. Liem, & D. B. Wake (Eds.), *Functional vertebrate morphology* (pp. 1–25). Cambridge, MA: Belknap Press.

Larson, S. G., Schmitt, D., Lemelin, P., & Hamrick, M. (2000). Uniqueness of primate forelimb posture during quadrupedal locomotion. *American Journal of Physical Anthropology*, *112*, 87–101.

Lee, K. C. L., & Lanyon, L. E. (2004). Mechanical loading influences bone mass through estrogen receptor α. *Exercise and Sport Sciences Reviews*, *32*, 64–68.

Lee, T. C., Staines, A., & Taylor, D. (2003). Bone adaptation to load: Microdamage as a stimulus for bone remodeling. *Journal of Anatomy*, *201*, 437–446.

Lieberman, D. E., & Pearson, O. M. (2001). Trade-off between modeling and remodeling responses to loading in the mammalian limb. *Bulletin of the Museum of Comparative Zoology*, *156*, 269–282.

Lieberman, D. E., Pearson, O. M., Polk, J. D., Demes, B., & Crompton, A. W. (2003). Optimization of bone growth and remodeling in response to loading in tapered mammalian limbs. *Journal of Experimental Biology A*, *206*, 3125–3138.

Main, R. P., & Biewener, A. A. (2004). Ontogenetic patterns of limb loading. *In vivo* bone strains and growth in the goat radius. *Journal of Experimental Biology*, *207*, 2577–2588.

Main, R. P., & Biewener, A. A. (2007). Skeletal strain patterns and growth in the emu hindlimb during ontogeny. *Journal of Experimental Biology*, *210*, 2676–2690.

Martin, R. B. (1974). *Prosimian biology*. London: Gerald Duckworth & Co Ltd.

Martin, R. B., & Burr, D. (1982). A hypothetical mechanism for the stimulation of osteonal remodeling by fatigue damage. *Journal of Biomechanics*, *15*, 137–139.

Merkens, H. W., Schamhardt, H. C., van Osch, G. J. V. M., & Bogert, A. J. (1993a). Ground reaction force patterns of dutch warmblood horses at normal trot. *Equine Veterinary Journal*, *25*, 134–137.

Merkens, H. W., Schamhardt, H. C., van Osch, G. J. V. M., & Hartman, W. (1993b). Ground reaction force patterns of dutch warmblood horses at canter. *American Journal of Veterinary Research*, *54*, 670–674.

O'Neill, M. C., & Schmitt, D. (2012). The gaits of primates: Center of mass mechanics in walking, cantering and galloping ring-tailed lemurs, *Lemur catta*. *Journal of Experimental Biology*, *215*, 1728–1739.

Oxnard, C. E., Crompton, R. H., & Lieberman, S. S. (1990). *Animal lifestyles and anatomies: The case of the Prosimian Primates*. Seattle, London: University of Washington Press.

Parr, W. C. H., Wroe, S., Chamoli, U., Richards, H. S., McCurry, M. R., Clausen, P. D., & McHenry, C. (2012). Toward integration of geometric morphometrics and computational biomechanics: New methods for 3D virtual reconstruction and quantitative analysis of finite element models. *Journal of Theoretical Biology*, *301*, 1–14.

Revell, L. J. (2012). Phytools: An R package for phylogenetic comparative biology (and other things). *Methods in Ecology and Evolution*, *3*, 217–223.

Riggs, C. M., Vaughn, L. C., Evans, G. P., Lanyon, L. E., & Boyde, A. (1993). Mechanical implications of collagen fibre orientation in cortical bone of the equine radius. *Anatomy and Embryology*, *187*, 239–248.

Riskin, D. K., Bertram, J. E., & Hermanson, J. W. (2005). Testing the hindlimb-strength hypothesis: Non-aerial locomotion by Chiroptera is not constrained by the dimensions of the femur or tibia. *Journal of Experimental Biology*, *208*, 1309–1319.

Robling, A. G., Hinant, F. M., Burr, D. B., & Turner, C. H. (2002). Improved bone structure and strength after long-term mechanical loading is greatest if loading is separated into short bouts. *Journal of Bone and Mineral Research*, *17*, 1545–1554.

Robling, A. G., Castillo, A. B., & Turner, C. H. (2006). Biomechanical and molecular regulation of bone remodeling. *Annual Review of Biomedical Engineering*, *8*, 455–498.

Rohlf, F. J., & Corti, M. (2000). Use of two-block partial least-squares to study covariation in shape. *Systematic Biology*, *49*, 740–753.

Rohlf, F. J., & Slice, D. (1990). Extensions of the Procrustes method for the optimal superimposition of landmarks. *Systematic Biology*, *39*, 40–59.

Rose, M. D. (1973). Quadrupedalism in primates. *Primates*, *14*, 337–357.

Rose, M. D. (1988). Another look at the anthropoid elbow. *Journal of Human Evolution*, *17*, 193–224.

Rubin, C. T., & Lanyon, L. E. (1984). Dynamic strain similarity in vertebrates; an alternative to allometric limb bone scaling. *Journal of Theoretical Biology*, *107*, 321–327.

Rubin, C. T., Gross, T. S., Donahue, H. J., Guilak, F., & McLeod, K. J. (1994). Physical and environmental influences on bone formation. In C. Brighton, G. Friedlander, & J. Lane (Eds.), *Bone formation and repair* (pp. 61–78). Rosemont, IL: American Academy of Orthopaedic Surgeons.

Ruff, C., Holt, B., & Trinkaus, E. (2006). Who's afraid of the big bad Wolff?: "Wolff's law" and bone functional adaptation. *American Journal of Physical Anthropology*, *129*(4), 484–498.

Schlager, S. (2013). *Morpho: Calculations and visualizations related to geometric Morphometrics. R Package Version* (pp. 21–1141011). Vienna, Austria: The R Foundation for Statistical Computing.

Schmitt, D. (1999). Compliant walking in primates. *Journal of Zoology*, *248*, 149–160.

Schmitt, D. (2003). Insights into the evolution of human bipedalism from experimental studies of humans and other primates. *Journal of Experimental Biology*, *206*, 1437–1448.

Schmitt, D., & Hanna, J. B. (2004). Substrate alters forelimb to hindlimb peak force ratios in primates. *Journal of Human Evolution*, *46*, 239–254.

Schmitt, D., & Lemelin, P. (2002). Origins of primate locomotion: Gait mechanics of the woolly opossum. *American Journal of Physical Anthropology*, *118*, 231–238.

Schmitt, D., & Lemelin, P. (2004). Locomotor mechanics of the slender Loris (*Loris tardigradus*). *Journal of Human Evolution*, *47*, 85–94.

Schmitt, D., Zumwalt, A. C., & Hamrick, M. W. (2010). The relationship between bone mechanical properties and ground reaction forces in normal and hypermuscular mice. *Journal of Experimental Zoology A*, *313*, 339–351.

Smith, J. M., & Savage, R. J. G. (1956). Some locomotory adaptations in mammals. *Zoological Journal of the Linnean Society*, *42*, 603–622.

Vilensky, J. A., & Larson, S. G. (1989). Primate locomotion: Utilization and control of symmetrical gaits. *Annual Review of Anthropology*, *18*, 17–35.

Wiley, D. F., Amenta, N., Alcantara, D. A., Ghosh, D., Kil, Y. J., Delson, E., ... Hamann, B. (2005). Evolutionary morphing. In Proceedings of IEEE Visualization 2005 (VIS'05), 23–28 October, 2005 Minneapolis, MN.

Zelditch, L. M., Swiderski, D. L., & Sheets, H. D. (2012). Partial least squares analysis. In *Geometric Morphometrics for biologists, a primer* (2nd ed., pp. 169–188). New York and London: Academic Press.

SUPPORTING INFORMATION

Additional supporting information may be found online in the Supporting Information section at the end of the article.

How to cite this article: Fabre A-C, Granatosky MC, Hanna JB, Schmitt D. Do forelimb shape and peak forces covary in strepsirrhines? *Am J Phys Anthropol*. 2018;167:602–614. https://doi.org/10.1002/ajpa.23688